Predicting MGMT Promoter Methylation of Glioblastoma from Dynamic Susceptibility Contrast Perfusion: A Radiomic Approach

Girolamo Crisi, Silvano Filice

From the Neuroradiology Unit, Azienda Ospedaliero-Universitaria of Parma, Parma, Italy (GC); Medical Physics Unit, Azienda Ospedaliero-Universitaria of Parma, Parma, Italy (SF).

ABSTRACT

BACKGROUND AND PURPOSE: **This study aims to investigate whether radiomic quantitative image features (IFs) from perfusion dynamic susceptibility contrast magnetic resonance imaging (DSC-MRI) retain sufficient strength to predict O6-methylguanine–DNA methyltransferase promoter methylation (MGMT_pm) in newly diagnosed glioblastoma (GB) patients.**

METHODS: **We retrospectively reviewed the perfusion DSC-MRI of 59 patients with GB. Patients were classified into three groups: (1) unmethylated if MGMT_pm ≤ 9% (UM); (2) intermediate-methylated if MGMT_pm ranged between 10% and 29% (IM); (3) methylated if MGMT_pm ≥ 30% (M). A total of 92 quantitative IFs were obtained from relative cerebral blood volume and relative cerebral blood flow maps. The Mann-Whitney U-test was applied to assess whether there were statistical differences in IFs between patient groups. Those IFs showing significant difference between two patient groups were termed relevant IFs (rIFs). rIFs were uploaded to a machine learning model to predict the MGMT_pm.**

RESULTS: **No rIFs were found between UM and IM groups. Fourteen rIFs were found among UM-M, IM-M, and (UM + IM)-M groups. We built a multilayer perceptron deep learning model that classified patients as belonging to UM + IM and M group. The model performed well with 75% sensitivity, 85% specificity, and an area under the receiver-operating curve of .84.**

CONCLUSION: **rIFs from perfusion DSC-MRI are potential biomarkers in GBs with a ≥30% MGMT_pm. Otherwise, unmethylated and intermediate-methylated GBs lack of rIFs. Five of 14 rIFs show sufficient strength to build an accurate prediction model of MGMT_pm.**

Keywords: Radiomics, dynamic susceptibility contrast MRI, perfusion, MGMT promoter methylation, glioblastoma.

Acceptance: Received March 26, 2020, and in revised form April 21, 2020. Accepted for publication April 21, 2020.

Correspondence: Address correspondence to Silvano Filice, Medical Physics Unit, Azienda Ospedaliero-Universitaria, via Gramsci 14, 43126 Parma, Italy. E-mail: sfilice@ao.pr.it.

Acknowledgments and Disclosure: The authors thank Virginia Grandi, trainee teacher of modern foreign languages at St. Helena School in Colchester (UK), for her linguistic assistance. This research received no external funding. The authors declare no conflicts of interest.

J Neuroimaging 2020;0:1-5.
DOI: 10.1111/jon.12724

Introduction

Radiomics is defined as the high throughput extraction of quantitative imaging features (IFs) from different imaging modalities and is much more efficient than conventional or nonradiomics methods of image analysis.[1-3] There is increasing evidence in neuro-oncology that combining radiomic features with magnetic resonance imaging (MRI) can provide insight into molecular subtype of glioblastoma (GB).[4-8] It is currently accepted that the methylation of the MGMT promoter (O6-methylguanine–DNA methyltransferase) is a favorable prognostic factor in patients with GB through a better response to temozolomide-based chemotherapy.[9,10] Several radiomics and nonradiomics studies have shown the potential of MRI to predict the MGMT promoter methylation (MGMT_pm).[11-16] Only two nonradiomics studies[17,18] using perfusion dynamic susceptibility contrast MRI (DSC-MRI) were attempting to investigate the relationship between the relative cerebral blood volume (rCBV) and MGMT_pm in GB patients. To date, the possibility of predicting the MGMT_pm from perfusion DSC-MRI using a radiomic approach has not been fully tested. The purpose of this study was to investigate whether IFs from perfusion DSC-MRI retain sufficient strength to predict MGMT_pm in newly diagnosed GB patients.

Methods

Patient Population

We retrospectively enrolled 59 patients with GB between June 1, 2013 and December 31, 2017 (Table 1). According to Dunn et al,[19] GBs were classified into three groups: (1) unmethylated if MGMT_pm ≤ 9% (UM); (2) intermediate-methylated if MGMT_pm ranged between 10% and 29% (IM); and (3) methylated if MGMT_pm ≥ 30% (M).

Inclusion criteria were: (1) MRI, including contrast-enhanced-T1-weighted (CE-T1W) images and perfusion DSC-MRI before initial surgery, radiation and chemotherapy; (2) newly diagnosed histologically confirmed GB; (3) patients >18 years of age; (4) IDH wild-type; and (5) MRI with no artifacts. The time to surgery was 2-7 days for 86% of patients. All the patients did not receive treatment with dexamethasone at the time of imaging. The study got approval from local ethical committee.

MRI

MRI was performed on a 3.0T whole body scanner (Discovery MR 750; GE Healthcare, Milwaukee, WI) equipped with an 8-channel phased-array head coil. Our MRI protocol for

Table 1. Patient Demographics

	GB Groups		
Parameter	**UM**	**IM**	**M**
Patients number	21	18	20
Age mean (range)	61.0 (31-73)	57.8 (39-70)	59.1 (32-77)
M (F)	13 (8)	12 (6)	14 (6)

UM = unmethylated GBs (MGMT_pm ≤ 9%); IM = intermediate-methylated GBs (MGMT_pm ranging between 10% and 29%); M = methylated GBs (MGMT_pm ≥ 30%); MGMT_pm = O6-methylguanine–DNA methyltransferase promoter methylation; M = male; F = female.

neuro-oncological applications includes 3-dimensional T1-weighted gradient-echo (T1GRE) sagittal images, axial T2 FLAIR images, axial T2 GRE images, and axial diffusion-weighted imaging (DWI). Perfusion DSC images were acquired using a gradient echoplanar imaging (EPI) sequence after administration of a compact bolus of gadoterate meglumine at a rate of 7 mL/second via a power injector through an 18-g intravenous line. The contrast bolus was followed by a saline flush of up to 20 mL at the same flow rate of a full dose (.1 mmol/kg body weight). The perfusion DSC parameters were as follows: repetition time (TR) = 1,500 milliseconds, echo time (TE) = 30 milliseconds, flip angle = 60°, field of view (FOV) = 24 × 24 cm, acquisition matrix = 128 × 128, voxel size = .9 × .9 × 1.0 mm, contiguous 4-mm-thick axial slices, and number of excitations = 1. Sixty phases were acquired, resulting in 1,320 images over a scan time of 90 seconds, corresponding to a temporal resolution of 1.5 seconds. Contrast media was administered with a fixed delay of 20 seconds after the start of the sequence in order to obtain sufficient pre-contrast images to define the baseline of the signal to time curve. Perfusion DSC was followed by 2-dimensional contrast-enhanced axial T1W-FSE (CE-T1W) and 3-dimensional sagittal T1GRE post-contrast images with the same parameters.

DNA Samples

The genomic DNA was extracted and purified from 5 micron sections of formalin-fixed paraffin-embedded tissue samples using the MagCore Genomic DNA Tissue kit and the Magcore F16 Plus Automated extractor (RBC Bioscience Corp., Taipei, TW). The DNA concentration was assessed by Quantus fluorometer with the Quantifluor ONE dsDNA System (Promega, Madison, Wisconsin, USA). Approximately 200-500 ng total DNA was subjected to bisulfite conversion and pyrosequencing analysis using the MGMT plus kit (Diatech Pharmacogenetics, Italy) and the PyroMark Q96 ID system (Qiagen, Valencia, CA, USA). Pyrosequencing yields data for 10 CpG sites within the MGMT promoter. For data analysis, the methylation percentage obtained for each CpG was averaged out across the 10 CpGs. According to Dunn et al,[19] GBs were considered methylated (M) if they had an average methylation 30% or unmethylated if ≤9% (UM). Average methylation ranging between 10% and 29% was considered as intermediate (IM).

DSC Processing

DSC data were processed using commercially available software NordicICE (DSC Module v. 4.1.2, NordicNeurolab, Bergen, Norway). This software application uses a fully automated pixel searching algorithm for arterial input function (AIF) detection. The AIF was obtained by drawing a small region of interest over the proximal middle cerebral artery. The effects of contrast agent extravasation due to blood-brain disruption were automatically corrected by fitting the dynamic data with the gamma variate function. The maps of rCBV and rCBF were generated automatically.

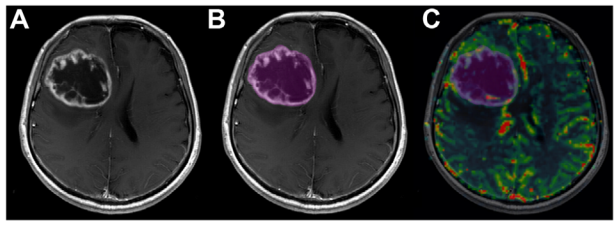

Fig. 1. A 49-year-old man with right frontal glioblastoma. (A) Contrast-enhanced-T1-weighted (CE-T1W) image. (B) CE-T1W image with region of interest (purple area) including enhancing tumor and necrotic core. (C) Cerebral blood volume map co-registered to CE-T1W image.

Image Analysis and Radiomic Features

Radiomic analysis has been accomplished with the open-source software packages LIFEx[20] (version 4.7; Orsay, France). A neuroradiologist with 20 years of experience who was blinded to the clinical and pathological data defined the volume of analysis (VOI). The neuroradiologist manually delineated the outer edge of tumor enhancing area, including the inner necrotic tumor, on every CE-T1W image (Fig 1). Care was taken to exclude surrounding normal brain vessels. VOI delineation required about 30-35 minutes for each patient and was the most time-consuming task. The rCBV and rCBF maps were co-registered to CE-T1W images. No image filtering was applied. For the purpose of IFs extraction: (1) all images used in this study were resampled to a voxel size of 2 × 2 × 4 mm^3; (2) the pixel values within the VOI were rescaled between the minimum and maximum value; (3) pixel values were discretized by applying a fixed bin size of 30. For each patient, a total of 92 IFs has been extracted from rCBV and rCBF maps. IFs included[21]: (1) shape features, describing geometrical characteristics of VOI; (2) first-order features, such as maximum, minimum, mean and standard deviation of pixels intensity value into the VOI; (3) histogram statistics describing the shape of the histogram of pixel intensity values into the VOI; (4) second-order features describing the spatial distribution of pixel intensities. The second-order features were derived from gray-level co-occurrence matrix, gray-level run length matrix, neighborhood gray-level dependence matrix, and gray-level zone length matrix.

Statistical Analysis

The statistical analysis has been carried out using the SPSS v. 20.0 software package. The two-tailed Mann-Whitney U-test was applied to assess whether there were differences in IFs between the following combinations of patient groups: (1) UM versus IM; (2) UM versus M; (3) UM versus (IM + M); (4) IM versus M; (4) (UM + IM) versus M. *P*-value of less than .05, adjusted for Bonferroni, was considered to indicate a statistically significant difference. Those IFs showing significant difference between two patient groups were termed relevant

Table 2. Summary of Relevant Image Features Extracted from Dynamic Susceptibility Contrast Perfusion Maps

DSC Map	rIF	Type of Feature	rIF Uploaded to MLP
rCBV	Conventional mean	First order	X
	Conventional std	First order	
	HISTO entropy	First order	
	GLCM energy	Second order	X
	GLCM contrast	Second order	
	GLCM entropy	Second order	X
	GLRLM SRLGE	Second order	X
	GLRLM SRHGE	Second order	
	NGLDM Busyness	Second order	
	GLZLM SZLGE	Second order	
rCBF	HISTO skewness	First order	X
	HISTO energy	First order	
	GLCM entropy	Second order	
	GLRLM SRHGE	Second order	

The relevant image features (rIFs) were shared among UM-M, IM-M, and (UM + IM)-M groups. rIFs are those features showing a significant difference between patients groups ($P < .05$). A subset of 5 of 14 rIFs were uploaded to a multilayer perceptron deep learning predictive model. To build the model, we considered two different groups belonging to UM + IM patients and M patients. rCBV = relative cerebral blood volume; rCBF = relative cerebral blood flow; UM = unmethylated GBs (MGMT_pm ≤ 9%); IM = intermediate-methylated GBs (MGMT_pm ranging between 10% and 29%); M = methylated GBs (MGMT_pm ≥ 30%); GB = glioblastoma; MLP = multilayer perceptron.

IFs (rIFs). To eliminate redundancy, the Spearman correlation test was applied to exclude correlated rIFs. Naïve Bayes (NB), Decision Trees (DT), and the multilayer perceptron (MLP) machine learning methods were employed to formulate a model to predict the MGMT_pm. The models were simulated using the open source software packages WEKA[22] ver. 3.8.3. A dedicated algorithm was applied to select a subset of rIFs to build each model. The models' performances were evaluated on the basis of a 10-fold cross-validation resampling procedure by assessing: area under the receiver-operating characteristic curve (AUC), sensitivity, and specificity.

Results

There were no significant differences between the patients' groups in terms of age and gender. No rIFs were found between UM and IM groups. Several rIFs were found among UM-M, IM-M, and (UM + IM)-M groups. After the Spearman correlation test, we selected 14 rIFs shared among UM-M, IM-M, and (UM + IM)-M groups (Table 2). To build a predictive model, we considered two different groups belonging to (UM + IM) patients and M patients. The best prediction power was obtained by using an MLP deep learning model and a subset of 5 of 14 rIFs as shown in Table 2. Box plot of subset of 5 rIFs is shown in Figure 2. Sensitivity, specificity, and AUC of the MPL deep learning model were: 75.0% (95% CI: 51.9-91.3%), 85.0% (95% CI: 70.2-94.3%), and .84, respectively. Figure 3 refers to the receiver-operating characteristic (ROC) curve for the model.

Discussion

Radiomics employs data-characterization algorithms to extract image features (IFs). Specifically, radiomics involves delineation of a volume of interest (VOI) on images, followed by computation of the quantitative features of the VOI and the voxels within it. IFs express the image properties,[1-3] and are generally categorized according to the level of complexity into: (1) shape features: describing geometrical properties of the VOI; (2) first-order features: describing the distribution of pixel intensities within the VOI; (3) second-order features: providing a measure of the spatial arrangement of the neighboring pixel intensities; (4) higher order features: obtained after applying filters or mathematical transform to the images (eg, wavelet transform, Laplacian transform, Gaussian filter, etc.). Radiomics is much more efficient than conventional or handcraft-based methods of image analysis, as it produces a large amount of IFs. Statistical analysis or dedicated selection algorithms are therefore required to: (1) identify the rIFs, namely those features that may be related to molecular signature of GB and (2) eliminate redundant features that are highly correlated to one another.[23] Nonredundant rIFs are suitable to be uploaded to a machine learning model for predicting molecular profiles.

Several radiomics and nonradiomics IFs from MRI have been used to characterize GBs, to describe molecular signature and to predict therapeutic response and patients' survival.[4-8] The MGMT_pm has been widely studied as a major predictor of GB response to temozolomide-based chemotherapy.[9,10] A recent review[24] systematically evaluated the performance of MRI to predict MGMT_pm in patients with newly diagnosed GB. The review included nonradiomics and radiomics MRI studies based on T1/T2-weighted images, CE-T1W images, FLAIR (fluid attenuated inversion recovery) and diffusion-weighted images. Nonradiomics studies were based on shape and first-order IFs, whereas radiomics also included higher order IFs. The review concluded that MRI have the potential to predict MGMT_pm with a pooled summary sensitivity and specificity of 79% and 78%, respectively. Furthermore, only two nonradiomic perfusion DSC-MRI studies[14,15] were conducted to investigate the relationship between rCBV values and MGMT_pm in a cohort of GBs but their results were controversial. One study[14] observed low rCBV values in methylated GBs, whereas the other one[15] reported no significant rCBV differences between unmethylated and methylated GBs. As the main result of the current study, we observed that 14 first- and second-order IFs were significantly different according to whether MGMT_pm was ≥30% or <30% (Table 2). Of these, 10 IFs were extracted from rCBV maps and four IFs from rCBF maps. Therefore, rCBV maps seem to offer more possibilities in terms of MGMT_pm determination. It has to be emphasized, however, that the rCBV value is just one of rIFs. Although the first-order feature rCBV mean value was lower in cases with methylation ≥30%, a comparison with the above studies was not possible since they did not report the cutoff to discriminate between unmethylated and methylated GBs. A recent multicenter nonradiomic perfusion DSC-MRI study including 184 patients with GB highlighted a strong association between overall survival (OS) and lower rCBV values.[25] Accordingly, our results also indicate that the reliability and consistency of rCBV alone in GBs would be improved if supported by or related to methylation percentage data. Only in this way we believe that rCBV values can become effective predictors of MGMT_pm in future MRI studies. In many neuro-oncological centers, the cutoff to discriminate between unmethylated and methylated GBs is 9–10%,[26] although there is no consensus on this threshold value. It has been reported that MGMT_pm ranging between 10% and 30% constitutes

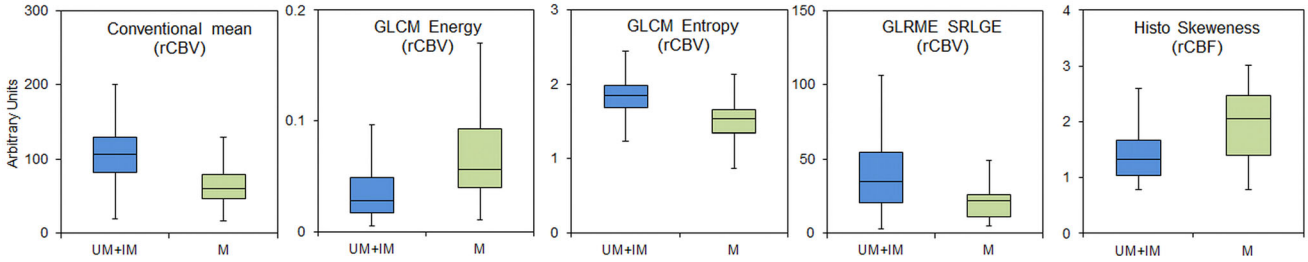

Fig. 2. Box plot of the 5 of 14 selected relevant image features to be uploaded to a multilayer perceptron deep learning model to predict MGMT_pm. UM = unmethylated GBs (MGMT_pm ≤ 9%); IM = intermediate-methylated GBs (MGMT_pm ranging between 10% and 29%); M = methylated GBs (MGMT_pm ≥ 30%).

a "gray zone" where the patient outcome is often different from what might be expected.[27,28] In their study regarding a cohort of 109 GBs treated with radio-chemotherapy, Dunn et al[19] demonstrated a significant difference in OS among IM, M, and UM groups. A large, multicenter, retrospective study of 376 GB patients[28] showed that a 24% methylation had a strong prognostic value in terms of OS. In other studies, a ≥30% methylation was associated with a median OS of 25.2 months compared to 15.2 months in all other patients.[29,30] Therefore, these findings indicate that methylation percentage plays an essential role in stratifying GB patients into poor and good prognostic groups. Unlike previous radiomic and nonradiomic MRI studies, we have added the molecular subclass UM, IM, and M of GB to image analysis. Thus, integrating the molecular subtype information, three different machine learning methods were adopted to predict the MGMT_pm of GBs. Setting a 30% MGMT_pm cutoff, the predictive models separated methylated GBs from unmethylated and intermediate methylated GBs (Fig 3). Focusing on a MLP deep learning model obtained by combining five rIFs, a satisfactory discriminatory power was achieved (AUC = .84). It should be emphasized that three of the five selected rIFs belonged to second-order type, showing that IFs describing the distribution of pixel intensities could play a pivotal role in the prediction of MGMT_pm. Anyway, it seems proved that IFs from perfusion DSC-MRI retain sufficient strength to predict MGMT_pm. Thus, the current study revealed that results of the radiomic analysis may be highly dependent on MGMT_pm cutoff. The revised 2016 edition of the WHO Classification of tumors of the central nervous system formally incorporated together molecular features and histology for classifying tumor type.[31] GBs have distinctive molecular features that are routinely analyzed in clinical practice and among these genetic biomarkers the MGMT_pm is one of the most important to be recognized. In the clinical setting, established molecular assays are required for MGMT_pm in order not to withhold temozolomide from patients who may potentially benefit from it, while sparing others in light of its toxicity and cost.[32] Using preoperative advanced MR imaging techniques like perfusion DSC-MRI, radiomic IFs may provide additional valuable information in quantifying the extent of methylation and are therefore important prognostic factors in patients with GB. A feature of GBs is cellular and molecular heterogeneity that causes a risk for sampling bias and patient stratification.[33] One of the main advantages of the radiomics is the ability to always perform a full analysis of the whole-tumor as the histopathological sampling cannot be representative of the entirety of the tumor and intratumoral heterogeneity can be

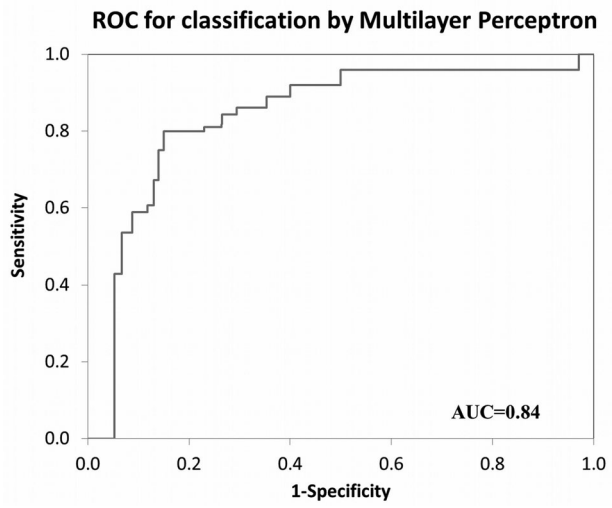

Fig. 3. Receiver-operating characteristic curve (ROC) for MGMT_pm prediction by multilayer perceptron deep learning algorithm based on 5 of 14 relevant image features. The ROC curve has been obtained by setting a 30% MGMT_pm cutoff to differentiate between UM + IM and M patients with GB. UM = unmethylated GBs (MGMT_pm ≤ 9%); IM = intermediate-methylated GBs (MGMT_pm ranged between 10% and 29%); M = methylated GBs (MGMT_pm ≥ 30%).

confusing for the neuropathologists. Therefore, perfusion DSC-MRI radiomics findings may be translated into the clinic for GB diagnosis when biopsy samples are inconclusive or in high-risk location.

Our study has several limitations. First, this is a single-center study based on onsite evaluation of a limited number of patients. Second, tissue perfusion may have differed between patients, increasing data variability. Third, the training samples available for MLP deep learning were limited and identical for testing. Fourth, UM + IM and M groups were imbalanced.

In conclusion, by integrating radiomics with perfusion DSC-MRI at the time of preoperative diagnosis, we have shown that first- and second-order rIFs are potential imaging biomarkers in GBs with a ≥30% MGMT_pm, which has been shown to have a highly significant predictive role of response to temozolomide-based chemotherapy. Otherwise, unmethylated and intermediate-methylated GBs lack of rIFs. Five of 14 rIFs show sufficient strength to build a prediction model of MGMT_pm that may be used by clinicians to provide prognostic data. The potential applications for radiomics are expanding in neuro-oncology given the opportunity to

noninvasively address diagnostic and prognostic decisive questions. Before clinical deployment, larger sample sizes with differentially methylated GBs should be conducted to further validate and improve the performance of the prediction model.

References

1. Rizzo S, Botta F, Raimondi S, et al. Radiomics: the facts and the challenges of image analysis. Eur Radiol Exp 2018;2:36.
2. Aerts HJ. The potential of radiomic-based phenotyping in precision medicine: a review. JAMA Oncol 2016;2:1636-42.
3. Lambin P, Rios-Velazquez E, Leijenaar R, et al. Radiomics: extracting more information from medical images using advanced feature analysis. Eur J Cancer 2012;48:441-6.
4. Sasaki T, Kinoshita M, Fujita K, et al. Radiomics and MGMT promoter methylation for prognostication of newly diagnosed glioblastoma. Sci Rep 2019;9:14435.
5. Bae S, Choi YS, Ahn SS, et al. Radiomic MRI phenotyping of glioblastoma: improving survival prediction. Radiology 2018;289:797-806.
6. Ellingson BM. Radiogenomics and imaging phenotypes in glioblastoma: novel observations and correlation with molecular characteristics. Curr Neurol Neurosci Rep 2015;15:506.
7. Li ZC, Bai H, Sun Q, et al. Multiregional radiomics features from multiparametric MRI for prediction of MGMT methylation status in glioblastoma multiforme: a multicentre study. Eur Radiol 2018;28:3640-50.
8. Prasanna P, Patel J, Partovi S, et al. Radiomic features from the peritumoral brain parenchyma on treatment-naïve multiparametric MR imaging predict long versus short-term survival in glioblastoma multiforme: preliminary findings. Eur Radiol 2017; 27:4188-97.
9. Florent Tixier , HyeminUm, DaltonBermudez, et al. Preoperative MRI-radiomics features improve prediction of survival in glioblastoma patients over MGMT methylation status alone. Oncotarget 2019;10:660-72.
10. Cabrini G, Fabbri E, Lo Nigro C, et al. Regulation of expression of O6-methylguanine-DNA methyltransferase and the treatment of glioblastoma (Review). Int J Oncol 2015;47:417-28.
11. Xi YB, Guo F, Xu ZL, et al. Radiomics signature: a potential biomarker for the prediction of MGMT promoter methylation in glioblastoma. J Magn Reson Imaging 2018;47:1380-7.
12. Kanas VG, Zacharaki EI, Thomas GA, et al. Learning MRI-based classification models for MGMT methylation status prediction in glioblastoma. Comput Methods Programs Biomed 2017;140: 249-57.
13. Drabycz S, Roldán G, de Robles P, et al. An analysis of image texture, tumor location, and MGMT promoter methylation in glioblastoma using magnetic resonance imaging. Neuroimage 2010;49:1398-405.
14. Levner I, Drabycz S, Roldan G, et al. Predicting MGMT methylation status of glioblastomas from MRI texture. Med Image Comput Assist Interv 2009;12:522-30.
15. Ahn SS, Shin NY, Chang JH, et al. Prediction of methylguanine methyltransferase promoter methylation in glioblastoma using dynamic contrast-enhanced magnetic resonance and diffusion tensor imaging. J Neurosurg 2014;121:367-73.
16. Korfiatis P, Kline TL, Coufalova L, et al. MRI texture features as biomarkers to predict MGMT methylation status in glioblastomas. Med Phys 2016;43:2835-44.
17. Ryoo I, Choi SH, Kim JH, et al. Cerebral blood volume calculated by dynamic susceptibility contrast-enhanced perfusion MR imaging: preliminary correlation study with glioblastoma genetic profiles. PLoS One 2013;8:e71704.
18. Kickingereder P, Bonekamp D, Nowosielski M, et al. Radiogenomics of glioblastoma: machine learning-based classification of molecular characteristics by using multiparametric and multiregional MR imaging features. Radiology 2016;281: 907-18.
19. Dunn J, Baborie A, Alam F, et al. Extent of MGMT promoter methylation correlates with outcome in glioblastomas given temozolomide and radiotherapy. Br J Cancer 2009;10: 124-31.
20. Nioche C, Orlhac F, Boughdad S, et al. LIFEx: a freeware for radiomic feature calculation in multimodality imaging to accelerate advances in the characterization of tumor heterogeneity. Cancer Res 2018;78:4786-9.
21. Nioche C, Orlhac F, Buvat I. Texture-user guide local image features extraction-LIFEx. Available at: www.lifexsoft.org/index.php/resources/documentation. Accessed March 23, 2020.
22. Witten H, Eibe F. *Data Mining: Practical Machine Learning Tools and Techniques*. 4th ed.Cambridge, MA: Morgan Kaufmann, 2017.
23. Gillies RJ, Kinahan PE, Hricak H. Radiomics: images are more than pictures, they are data. Radiology 2016;278:563-77.
24. Suh CH, Kim HS, Jung SC, et al. Clinically relevant imaging features for MGMT promoter methylation in multiple glioblastoma studies: a systematic review and meta-analysis. Am J Neuroradiol 2018;39:1439-45.
25. Álvarez-Torres MDM, Juan-Albarracín J, Fuster-Garcia E, et al. Robust association between vascular habitats and patient prognosis in glioblastoma: an international multicenter study. J Magn Reson Imaging 2020;51:1478-86.
26. Malmström A, Łysiak M, Kristensen BW, et al. Do we really know who has an MGMT methylated glioma? Results of an international survey regarding use of MGMT analyses for glioma. Neurooncol Pract 2020;7:68-76.
27. Wick W, Weller M, Van den Bent M, et al. MGMT testing the challenges for biomarker-based glioma treatment. Nat Rev Neurol 2014;10:372-85.
28. Lombardi G, Bellu L, Villani V, et al. A large, multicenter, retrospective study to identify a cutoff of MGMT methylation status by quantitative pyrosequencing approach in patients (PTS) with glioblastoma (GBM). J Clin Oncol 2018;36:2012-12.
29. Brigliadori G, Foca F, Dall'Agata M, et al. Defining the cutoff value of MGMT gene promoter methylation and its predictive capacity in glioblastoma. J Neurooncol 2016;128:333-9.
30. Gurrieri L, De Carlo E, Gerratana L, et al. MGMT pyrosequencing-based cut-off methylation level and clinical outcome in patients with glioblastoma multiforme. Future Oncol 2018;14: 699-707.
31. Louis DN, Perry A, Reifenberger G, et al. The 2016 World Health Organization classification of tumors of the central nervous system: a summary. Acta Neuropathol 2016;131:803-20.
32. Hegi ME, Genbrugge E, Gorlia T, et al. MGMT promoter methylation cutoff with safety margin for selecting glioblastoma patients into trials omitting temozolomide: a pooled analysis of four clinical trials. Clin Cancer Res 2019;25:1809-16.
33. Wenger A, Ferreyra Vega S, Kling T, et al. Intratumor DNA methylation heterogeneity in glioblastoma: implications for DNA methylation-based classification. Neuro Oncol 2019;21:616-27.